Digital Damage Detection Due to the 1999 Kocaeli, Turkey Earthquake

Miguel ESTRADA[1], Masashi MATSUOKA[2] and Fumio YAMAZAKI[3]

ABSTRACT

In this study, digital damage detection using remotely sensing images is applied to identify the affected areas due to the Kocaeli, Turkey earthquake of August 17,1999. The aim of this study is to identify the hard-hit areas in different levels of building damage, areas sunk into the sea and areas affected by fire. The analysis was carried out for Marmara Sea region, especially Gölcük city, where building damage and ground settlement were most prominent. The data used are optical remote sensing images taken by Landsat/TM satellite on March 27 and August 18, 1999, before and after the earthquake, respectively. In addition to these images, a set of images taken on September 3, 1999 is used to examine the identification method. For the detection of burned and sunk areas, a spectral comparison of the Landsat/TM is carried out. In order to detect the different levels of building damage in the urban area, a comparison of the ratio between different bands of the pre- and post-event images was conducted. The principal component analysis was further conducted for each pair of images and the results were compared. In order to calibrate the results of these comparisons, the product images were geographically corrected, and then they were compared with the ground truth data on GIS.

Key Words: *The 1999 Kocaeli earthquake, Landsat/TM, remote sensing, damage detection, building collapse, fire, subsidence.*

INTRODUCTION

The identification of damage due to large earthquakes is a vital issue to grasp the level and extension of the hard-hit areas. The evaluation can be conducted through a field reconnaissance survey. Even though the field survey has high accuracy, it requires a lot of resources and time. In the event of large natural disasters, like a destructive earthquake, a fast assessment of the damaged areas is required for rescue operations and emergency services. In a longer time span, the extension and degree of damage is vital information to outline restoration and reconstruction planning. Recently remote sensing technology has become a tool for identification of hard-hit areas after the occurrence of natural disasters like floods, landslides or earthquakes. Using Landsat/TM and SPOT/HRV images, Matsuoka and Yamazaki (1999) determined the areas suffered by fire, liquefaction, and building collapse due to the 1995 Kobe earthquake. This study provides a similar example of damage detection using satellite remote sensing for the Kocaeli, Turkey earthquake of August 17,1999. The location of different types of damage like fire outbreak, ground settlement and building damage using Landsat/TM data is considered.

[1] Graduate Student, Institute of Industrial Science, The University of Tokyo.
[2] Chief Research Engineer, Earthquake Disaster Mitigation Research Center, RIKEN.
[3] Associate Professor, Institute of Industrial Science, The University of Tokyo.

The basic premises in remote sensing based change detection are: the changes in land cover result in changes in radiance values, and the changes in radiance due to the land cover changes are large with respect to the radiance changes caused by other factors, such as atmospheric condition, soil moisture, and sun angle. In order to identify the different kind of damage, the comparison of optical satellite images taken before and after the earthquake is conducted. In this study the region along Marmara Sea, especially Gölcük city, where building damage and ground settlement were most prominent, were focused.

First, image-to-image registration was carried out to match the images. To detect the fire outbreak we compare the profiles along X and Y-axes of the pre- and post-event images. For the detection of the sunken area to the sea, the histograms of the infrared band are matched and then the resultant images are compared. For the detection of different levels of building damage, an analysis in the visible range is conducted as well as the principal component analysis.

Some general information about the 1999 Kocaeli Earthquake from U.S. Geological Survey and Kandili Observatory is: origin time: 00:01:38.56 (UTC), Mw = 7.4, epicenter: Lat. = 40.702N, Long. = 29.987E (Fig. 1), source depth= 17 km. According to the Government of Turkey, 17439 people were killed and 43953 were injured. 60000 to 115000 buildings were estimated to be collapsed or damaged beyond repair (EERI, 2000).

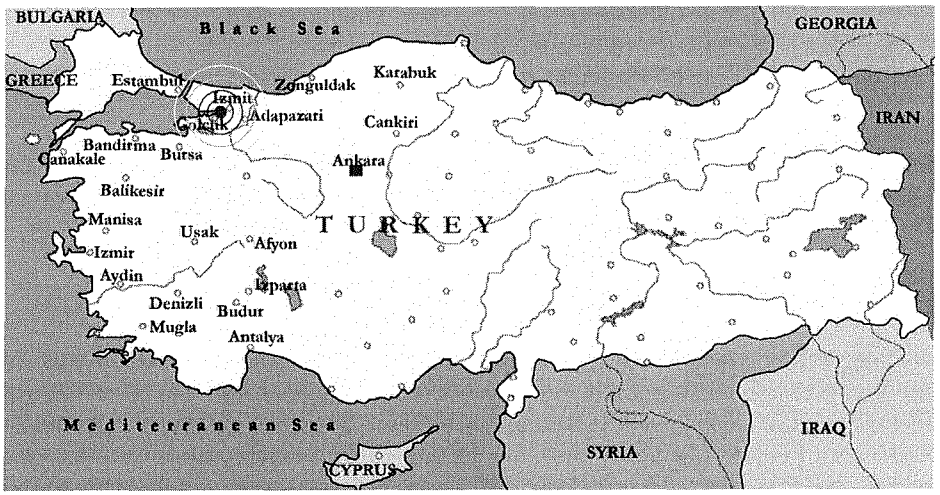

Figure 1. Map of Turkey and the epicenter of the earthquake.

LANDSAT/TM IMAGES

The data used in this research are remote sensing images from Landsat/TM satellite taken over the affected area before and after the earthquake. We analyzed the image that was taken on March 27, 1999 as a pre-event image, and those taken on August 18, and September 3, 1999 as post-event images. The composite color image (bands 751) one day after the earthquake (August 18, 1999) is shown in Figure 2. The image covers an area of 185 km by 154 km. Accurate spatial registration of the two images is essential for change detection. Therefore, the two sets of images, pre- and post-event, have to be registered; it means the pixels in both images must represent the same geographic location. To make an image-to-image registration, one of them is chosen as the master, to which the other, known as the slave,

is to be registered. In this study, the pre-event image is taken as the master and the post-event image is used as the slave. The image registration was conducted for the total area of the images by selecting 250 ground control points, deployed on the extension of the images. Rotation, scaling and translation method was used for warping the slave image and the nearest-neighbor method was employed for resampling.

Figure 2. Composite color image (Red=Band 7, Green=Band 5 and Blue=Band 1) of Landsat/TM taken on August 18, 1999 over Marmara Sea region.

IDENTIFICATION OF AREAS AFFECTED BY FIRE

To identify the areas affected by fire, we compared the profiles of the pre- and post-event images. The profile represents the distribution of the digital number (DN) of a certain band along a strip of the image. This strip can be taken over the X-axis or Y-axis. For this comparison, the band 5 (mid infrared), band 6 (far infrared or thermal band) and band 7 (mid infrared) were employed.

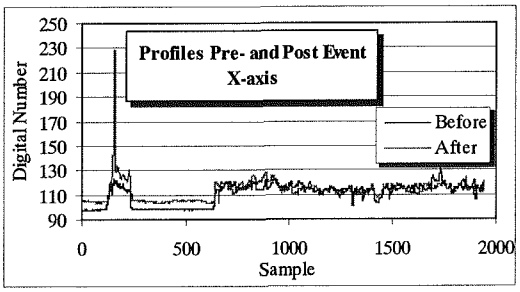

(a) Profile along X-axis.

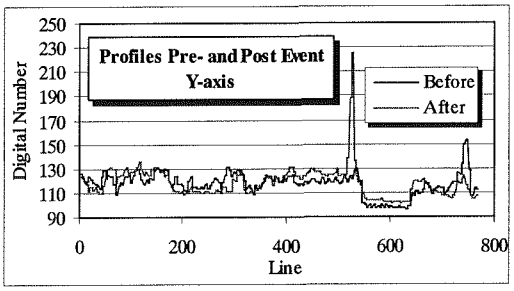

(b) Profile along Y-axis.

Figure 3. Digital number profiles of the pre- and post-event images of band 6. The peak values represent the area around Tüpras refinery, where a big fire broke out.

Figure 3 depicts the profiles of the DN of band 6 along the X and Y-axes. In the figure, a pattern in the profile before the earthquake can be observed as well in the after one. But in the region between sample 100 and sample 200, in the X-axis, and between the line 500 and 600, in the Y-axis, the peak values, which represent the high temperature, exist. Since the coordinates of this area are known, we can identify it in the image. This area corresponds to the Tüpras refinery, which was suffered from a large fire (MCEER, 2000). Figure 4 shows the close-ups of the composite color image (752) near the refinery before and after the event.

(a) Pre-event (March 27, 1999)

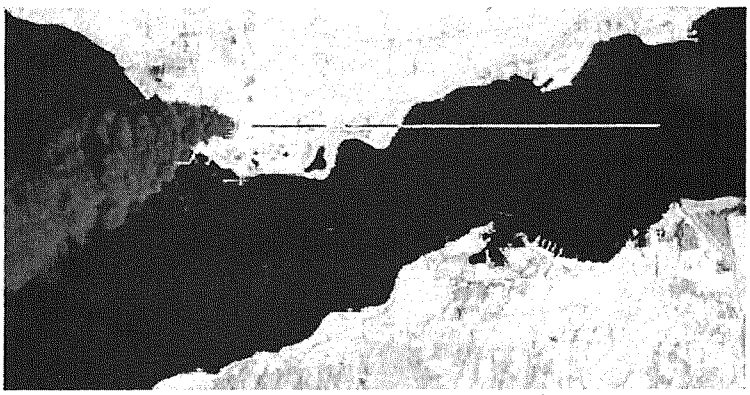

(b) Post-event (August 18,1999)

Figure 4. Color composite (752) images of Landsat/TM around Tüpras refinery.

IDENTIFICATION OF SUBSIDENCE AREAS IN GÖLCÜK CITY

Remote sensing provides a straightforward tool to map the extent of water bodies, to inventory an area occupied by open water, and to monitor changes in water bodies over time. Comparison of shoreline positions before and after flooding permits the measurement of the flooded area as well as the determination of location of the flooded area. Such information is difficult to acquire by conventional means. Determination of the land vs. water body is usually easiest in the near-infrared region, where land, especially if vegetated, is bright and open water dark (see Figure 5).

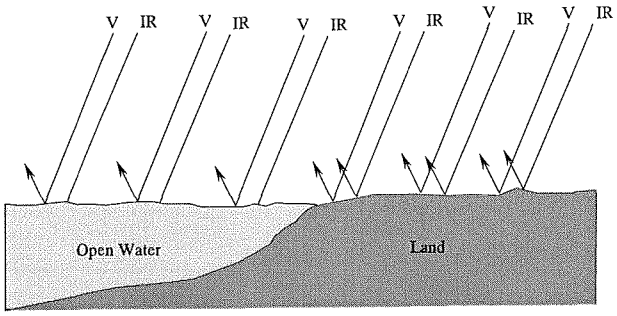

Figure 5. Identification of land-water contact (V: visible bands, IR: Infrared bands)

In order to detect the sunken areas, we matched the histograms (Figure 6) of the near-infrared band (band 4) of the two images (pre- and post-event). By matching the histograms of the two images corresponding to the area including Gölcük, we can obtain an apparent distribution of brightness as close as possible and can minimize the brightness value variations. Since the reflectance value of the water in the near infrared band is low, we matched the histograms in the range 1 to 20 (DN in Figure 6) and obtained the images shown in Figure 7. Comparing the two images, some areas that differ in the two time periods can be detected. These differences represent the water inundation. It is possible to calculate the extension of the flooding by counting the corresponding number of pixels. In order to count the number of pixels that belong to the water body, the 2-D scatter diagram showing the distribution of reflectance of two bands, in this case band 4 vs. band 5, was introduced. We defined threshold values for the reflectance of water, based on the values of water in the training area.

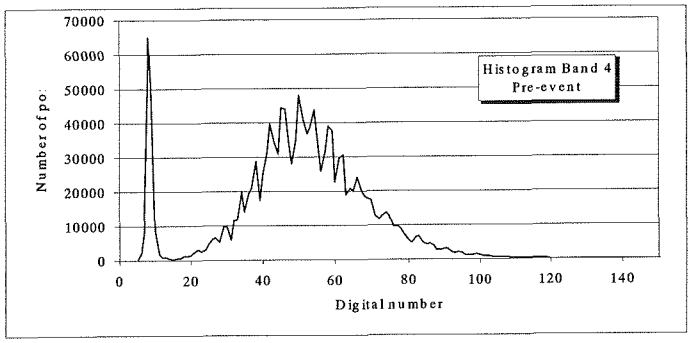

(a) Pre-event (March 27, 1999)

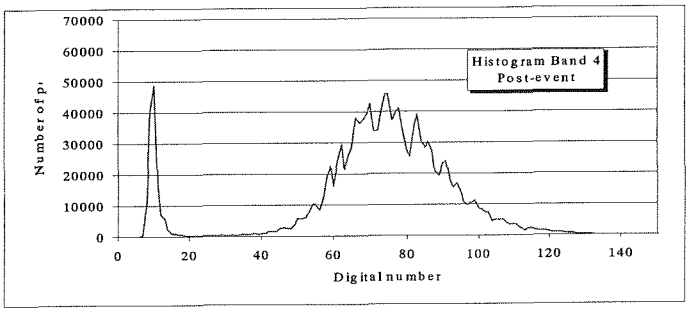

(b) Post-event (August 18,1999)

Figure 6. Histogram of the near infrared band near Gölcük

(a) Pre-event (March 27, 1999)

(b) Post-event (August 18,1999)

Figure 7. Coastline in Gölcük, after matching the histograms. As can be seen in the post-event image (b) in the upper-right part of the image is covered by water. The composite color image (321) was superposed to get better details of the area.

Landsat/TM images are composed of 30 m ground-resolution-cells for all of its bands (except band 6, which has 120 m resolution). If we take a difference of these two images, we can find the number of pixels that differ from one image to another. Multiplying the number of pixels obtained by this difference by the area of each pixel, we can obtain the total extent of the sunken area. Although this estimation is rather crude, it gives an idea of the extension of the damage.

With the threshold values shown in the Table 1 and the 2-D scatter diagrams shown in Figure 8, the number of pixels that belong to water before and after the event was obtained.

Number of pixels that belong to water: 8430 pixels (before), 9413 pixels (after),
Difference: 983 pixels.

Thus, the total sunk area is estimated as 983 x 30 x 30 = 884,700 m^2.

Table 1. Threshold values for bands 4 and 5, for the detection of sunken area

	Band 4		Band 5	
	Minimum	Maximum	Minimum	Maximum
Before EQ	0	10	0	13
After EQ	6	25	1	25

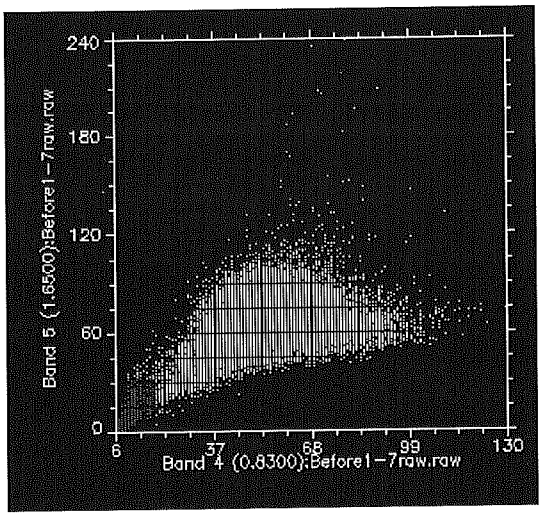

(a) pre-event (March 27, 1999)

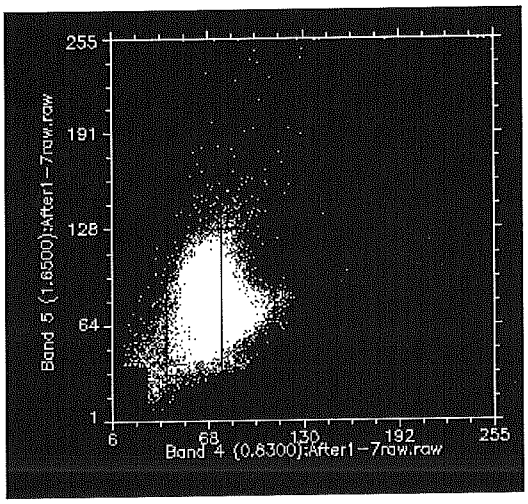

(b) post-event (August 18,1999)

Figure 8. 2-D Scatter diagram Band 4 vs. Band 5 for calculating sunk areas near Gölcük

IDENTIFICATION OF DIFFERENT LEVELS OF BUILDING DAMAGE

Comparison in the Visible Range

As a first comparison for the detection and localization of building damage, we conducted the comparison of the data in the visible range. For Landsat/TM satellite images, bands 1, 2 and 3 cover the visible range. First we calculate de average of these first three bands by the equation:

$$BR_{avg}(i,j) = \sum_{k=1}^{3} BB_k(i,j) \Big/ 3 \tag{1}$$

where $BB_k(i, j)$ is the digital number of the pixel (i, j) of the band k of the pre-event image, and $BR_{avg}(i, j)$ is the averaged value of the pixel (i, j) of the pre-event image. The similar equation is also applied to the post-event images. Then, we calculate the ratio between the two averaged images by Equation 2, where AR represents the averaged image after the event and R the ratio.

$$R(i,j) = AR_{avg}(i,j) / BR_{avg}(i,j) \tag{2}$$

Figure 9 shows the image obtained from this equation. In the center of the image, the damaged area appears brighter and the sunken area can be distinguished in dark tones. This image was then compared with the ground truth data (AIJ, 1999), shown in Figure 10. As a result of this comparison, the distribution of DN for the different levels of damage was obtained. Figure 11 shows 4 different damage categories: the sunk area (blue), low level building damage (green and turquoise), building damage ratio of 12.5% - 25% (yellow), and high level damage (read and orange). The order of the cumulative probability curves corresponds to the building damage severity, which means the debris has a higher reflectance in the visible region than the buildings in good condition.

Principal Component Analysis

The Principal Component Transformation is designed to reduce redundancy in multispectral data (Schowengerdt, 1997). The purpose is to compress all of the information contained in an original n-bands data set into fewer n new bands or *components*. Let $L=\{L_1(DN_k), L_2(DN_k)\}$ be a combined set of $2n$ bands images composed of two different dates images and C_L be the variance-covariance matrix of L. Each principal component X_j is expressed as

$$X_j = \sum_{k=1}^{n} \alpha_k L_1(DN_k) + \sum_{k=1}^{n} \beta_k L_2(DN_k) \tag{3}$$

where $\{\alpha_k, \beta_k\}$ is the normalized eigenvectors of the variance-covariance matrix C_L of L. Difference of the surface reflectance between two dates is evaluated by the following principal component:

$$D = \sum_{k=1}^{n} \alpha_k L_1(DN_k) + \sum_{k=1}^{n} \beta_k L_2(DN_k), (\alpha_k > 0, \beta_k < 0 \text{ for all } k) \tag{4}$$

In this case, by employing the 6 non-thermal bands of the pre- and post-event images, we obtain the $2n$ set. In this study the third principal component satisfies the condition given by Equation 4, where the first 6 coefficients are positives and the lasts 6 are negative. It means this principal component conveys the changes between the pre- and post-event images for this multitemporal set of images.

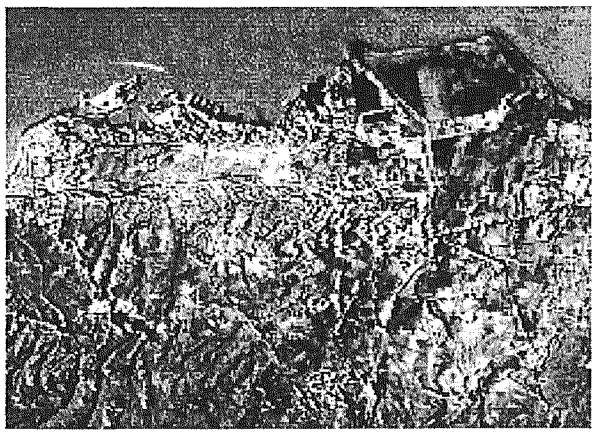

Figure 9. Ratio (after/before) of the average of the first three visible bands using March-August image pair

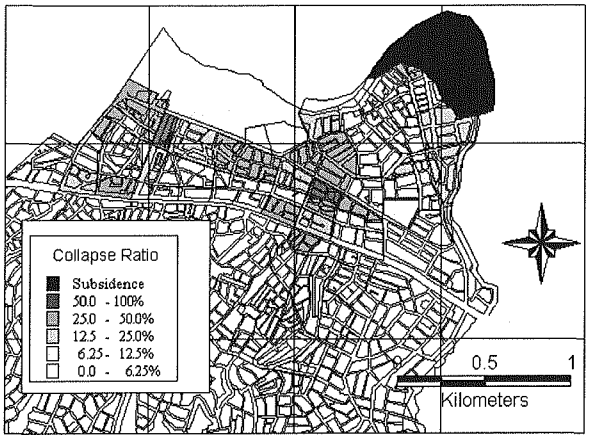

Figure 10. Building damage distribution in Gölcük city by the field survey of AIJ (1999)

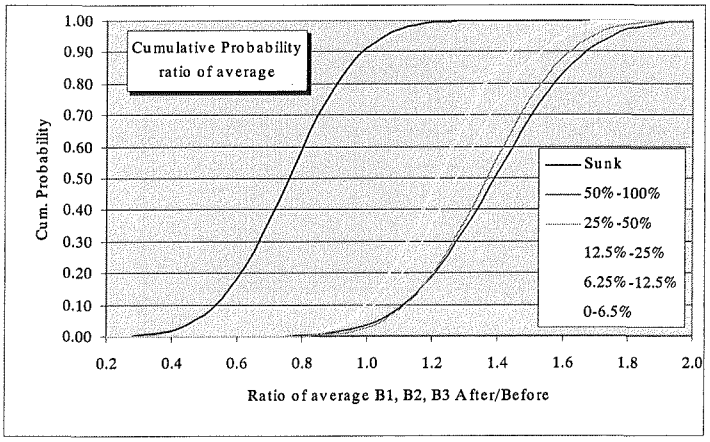

Figure 11. Cumulative probability of the ratio (after/before) of the averaged images using March-August image pair

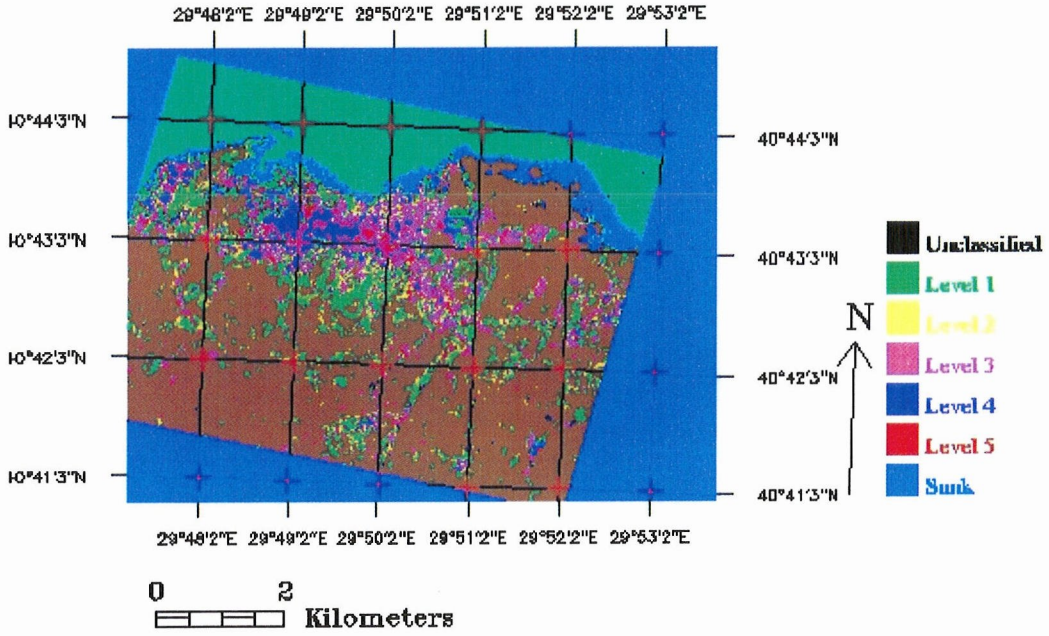

Figure 12. Spatial distribution of damage using the maximum likelihood classifier for Gölcük using March-August image pair

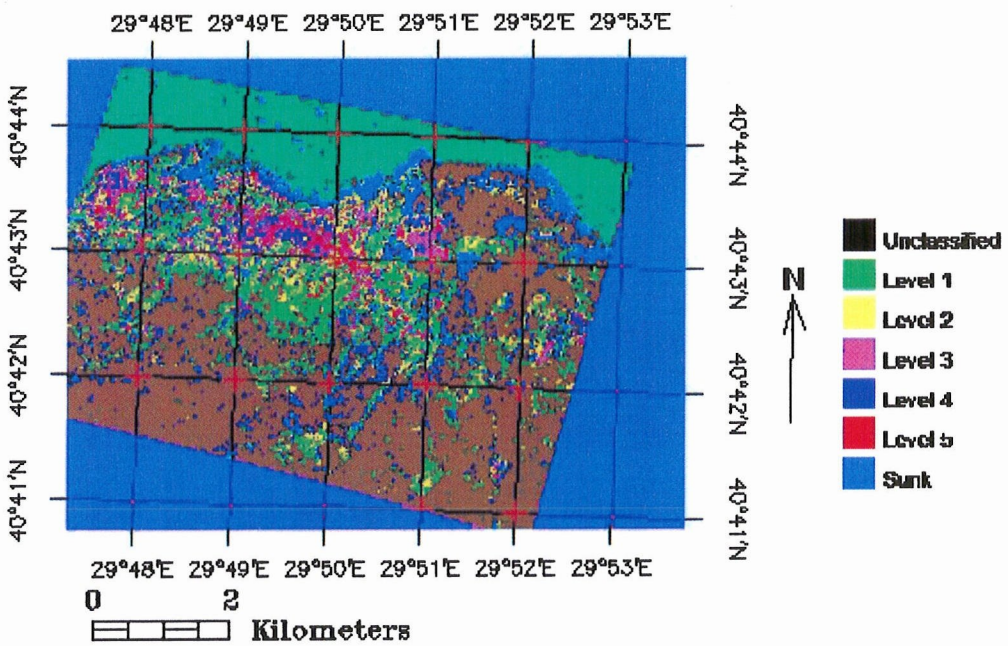

Figure 13. Spatial distribution of damage using the maximum likelihood classifier for Gölcük using March-September image pair

The digital number of the pixels for the third principal component image also follows the same distribution shown in Figure 11. Based on the distribution of the digital number and using the maximum likelihood classifier (Campbell, 1996), the spatial distribution of the building damage in Gölcük was obtained as shown in Figure 12. The figure shows the distribution of the different levels of damage from Level 1 (no damage) up to Level 5 (high level of damage) and the sunken area. This estimation seems to be in good agreement with the ground truth data shown in Figure 10. However, since the area covered by the field survey is rather limited, a further study may be required to discuss the accuracy of the estimated damage distribution from Landsat/TM data.

Examination of the Method using Another Post-event Image

As a test of the methodology, another post-event Landsat/TM image was employed. Landsat satellite has the return period of 16 days, and thus the next possible set of images is that acquired on September 3, 1999. Fortunately, the weather condition was favorable and good quality images were obtained.

The same procedure used for March-August image pair was employed to March-September image pair. The result of the analysis is shown in Figure 13. The estimated damage distribution from this new image pair looks very similar to that using March-August image pair shown in Figure 12. Note that the August image was taken one day after the earthquake. It is observed that the area corresponding to damage level 5 expanded compared with that from the previous image pair. This expansion of the hard-hit area, which means a big change in reflectance, is probably due to demolition and cleaning works after the earthquakes.

CONCLUSIONS

Digital damage detection due to the 1999 Kocaeli, Turkey earthquake was carried out using Landsat/TM satellite images, taken before and after the earthquake. Fire and sunk areas were successfully identified using the thermal band and the near infrared band, respectively. Compared with the result of the field survey in Gölcük by AIJ team, different levels of building damage were recognized properly. The digital numbers of the affected areas were observed to increase with the level of building damage going up. This fact corresponds the increase of reflectance in visible ranges due to the spread of debris after the earthquake. Applying the principal component analysis, we found that in case of Landsat/TM images, the third principal component conveys the changes in the multitemporal 12 non-thermal bands image. The method was further tested using another post event image.

This study provided the example of the use of Landsat/TM images to earthquake damage detection in a large area. Although the current investigation was constrained by the ground resolution of Landsat images, the result may be encouraging for the use of high-resolution optical satellites, e.g. IKONOS, to damage detection due to natural disasters.

REFERENCES

AIJ Reconnaissance Team, Kabeyasawa, T. et al. (1999). Progress Report on Damage Investigation after Kocaeli Earthquake by Architectural Institute of Japan. *Proc. ITU-IAHS International Conference on the Kocaeli Earthquake 17 August 1999.*

Campbell, J. (1996). *Introduction to Remote Sensing. Second Edition.* The Guilford Press. USA.

Earthquake Engineering Research Institute. (2000). Kocaeli, Turkey, Earthquake of August 17, 1999: Reconnaissance Report, *Earthquake Spectra.* Supplement A to Volume 16.

Matsuoka, M. and Yamazaki, F. (1999). Characteristics of Satellite Images of Damaged Areas due to the 1995 Kobe Earthquake. *2nd Conference on the Applications of Remote Sensing and GIS for Disaster Management*. The George Washington University, CD-ROM.

MCEER. (2000). *The Marmara, Turkey Earthquake of August 17, 1999: Reconnaissance Report*. Technical Report MCEER-00-0001.

Schowengerdt, R. (1997). *Remote Sensing, Models and Methods for Image Processing*. Academic Press. USA.